



# University of Kut Journal

ISSN (E): 2616 - 7808 II ISSN (P): 2414 - 7419 www.kutcollegejournal.alkutcollege.edu.iq k.u.c.j.sci@alkutcollege.edu.iq



Special Issue for the Researches of the 6th Int. Sci. Conf. for Creativity for 16-17 April 2025

# Valuation and Guess Single-phase transition to turbulent Developing Flows and Pressure Drop in a Copper Horizontal Pipe Heat Transfer by Using the Iterative Theory

Raed Shakir 1

#### **Abstract**

This study examines forced convection over smooth surfaces and horizontally arranged circular tubes, addressing various challenges. The primary aim is to analyze the heat transfer coefficient under specific forced convection conditions. Circular pipe test sections, each with an internal and external diameter of 0.009 meters and a total length of one meter, were used for evaluation. The working fluid, R113, entered at 25°C, with mass flow rates between 10 and 17.5 grams per second and heat inputs ranging from 25 to 100 watts. Reynolds numbers at the inlet and outlet varied within the ranges of 2115.80–2187.21, 2645.30–2789.30, 3174.79–3391.99, and 3704.28–3995.04. The research focused on the progression of transition and turbulent flow regions during all heat tests, tracking the expansion of laminar zones. An iterative prediction approach in Excel applied over 5,180 heat transfer corrections to determine the boundaries of these flow regions.

Keywords: single-phase, transition flow, turbulent flow, pressure drop, iterative Theory

# التقييم والتخمين الانتقال أحادي الطور من التدفقات النامية إلى المضطربة وانخفاض الضغط في أنبوب نحاسي أفقي ناقل للحرارة باستخدام النظرية التكرارية م. رائد شاكر <sup>1</sup>

#### المستخلص

تدرس هذه الدراسة الحمل الحراري القسري على الأسطح الملساء والأنابيب الدائرية المرتبة أفقيًا، متطرقة إلى تحديات متنوعة. الهدف الرئيسي هو تحليل معامل انتقال الحرارة في ظل ظروف حمل حراري قسري محددة. استخدمت مقاطع اختبار أنابيب دائرية، قطر كل منها داخلي وخارجي 0.009 متر وطول إجمالي متر واحد، التقييم. دخل سائل التشغيل، 1133، عند درجة حرارة 25 درجة مئوية، بمعدلات تدفق كتلة تتراوح بين 10 و17.5 غرام في الثانية، ومدخلات حرارية تتراوح بين 25 و100 واط. تراوحت أرقام رينولدز عند المدخل والمخرج بين في الثانية، ومدخلات درارية تتراوح بين 28 و17.50 و 3704.28 و 3391.09 و 3704.28 و 3995.04 و 3995.04 و المخرج بين البحث على تطور مناطق التدفق الانتقالي والمضطرب خلال جميع اختبارات الحرارة، مع تتبع توسع المناطق الصفائحية. وقد طبقت أكثر من 5180 تصحيحًا لانتقال الحرارة باستخدام نهج التنبؤ التكراري في برنامج إكسل لتحديد حدود مناطق التدفق هذه.

الكلمات المفتاحية: مرحلة واحدة، تدفق انتقالي، تدفق مضطرب، انخفاض الضغط، طريقة تكرارية

#### **Affiliation of Author**

<sup>1</sup> Petroleum and Gas Engineering Department, College of Engineering, University of Thi-Qar, Iraq, Thi-Qar, 64001

<sup>1</sup>raed-sh@utq.edu.iq

<sup>1</sup> Corresponding Author

Paper Info.

Published: Oct. 2025

ا**نتساب الباحث** أقسم هندسة النفط والغاز، كلية

الهندسة، جامعة ذي قار، العراق، ذي قار، 64001

<sup>1</sup> raed-sh@utq.edu.iq

1 المؤلف المراسل

معلومات البحث تأريخ النشر: تشرين الاول 2025

### Introduction

Flow inside a tube can be classified into developing transitional and developing turbulent states, where two distinct convection mechanisms occur. It is vital to differentiate among forced also mixed convection, as the Reynolds number plays a significant role in various scenarios. In turbulent

tube flow, mixed convection results from buoyancy-induced radial density variations, leading to the simultaneous presence of both convection types. Understanding these distinctions is particularly important when the Reynolds number is a key factor and boundary conditions involve a constant heat flux. While Alsayah, Ahmed Mohsen et al.[1], [2] analysed a heat pipe heat exchanger, developing an advanced numerical iterative method with predictive software to assess transmission characteristics forced heat in convection and liquid dynamics. B. K. Dutta, [3] and Holman [4],had used many heat transfer correlations that we have been developed them. Shakir. et al.[5–18] have extensively studied heat sinks, providing essential analytical and numerical insights for different configurations, including flat channels, pin-fin channels, and micro-channels. This study primarily focuses on predictive modelling, using heat transfer equations to replicate theoretical conditions resembling laboratory environments. Additionally, S. R. Nashee [19–21] investigated heat and mass This research transfer properties. employs predictive analysis and heat transmission equations to model theoretical conditions that reflect real laboratory experiments. It aims to establish an advanced numerical iterative framework by integrating prediction software with Excel and incorporating over 5,180 heat transfer correlations to evaluate heat transfer and fluid flow behaviour in forced convection. As depicted in Figure 2, heat transmission primarily takes place at the interface among solid surfaces besides air, allowing for the examination of boundary wall effects in both perpendicular and parallel orientations to airflow while considering thermal conductivity.

## The Rig

If a flow loop is established for developing the new technology illustrated in **Figure.2**, the process flow is represented schematically. Prior to each test, the R113 fluid undergoes degassing through intensive heating for approximately 3.5 hours to

eliminate dissolved gases, which are then vented into the atmosphere. To facilitate this, the vent valve at the top of the preheater is periodically opened, allowing gas to escape. Following degassing, a pressure test is performed to confirm the absence of gas or air bubbles in the fluid before initiating single-phase tests. The primary line regulates the required mass flow rate, starting with a coarse filter to remove larger debris. As the advances. finer filters enhance process purification. During testing, the R113 mass flow rate and inlet temperature (Tin) are adjusted for optimization, with the coarse filter trapping larger particles. A flow meter measures the mass flow rate (mT) before the fluid moves through a bypass valve and a control valve, eventually entering a horizontal heat tube. The controller modifies the applied heat based on the observed flow rate, ensuring precise thermal regulation as the R113 circulates through the system. The preheater maintains the required inlet temperature (Tin) for the copper housing of the horizontal heat tube. Integrated with the system controller, the preheater enables synchronized heater adjustments to sustain the necessary heat input. This process continues until the R113 fluid reaches a steady-state condition, typically requiring 2 to 3.5 hours. Stabilizing both the outlet temperature (Tout-th) and the housing wall temperature (Tw) is essential, with equilibrium generally achieved within 38 to 53 minutes. During single-phase testing, an iterative approach is used to keep system pressure aligned with ambient pressure by adjusting the heat rate accordingly. The testing phase concludes once all predefined procedures have been completed successfully as shown in Figure (1) and Figure (2).

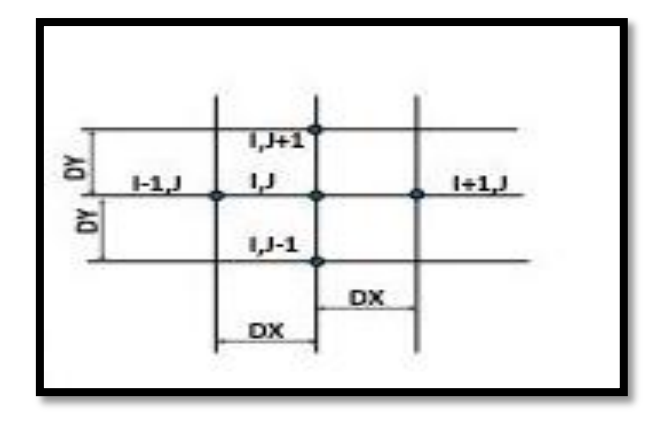


Figure (1): The square cells of pipe

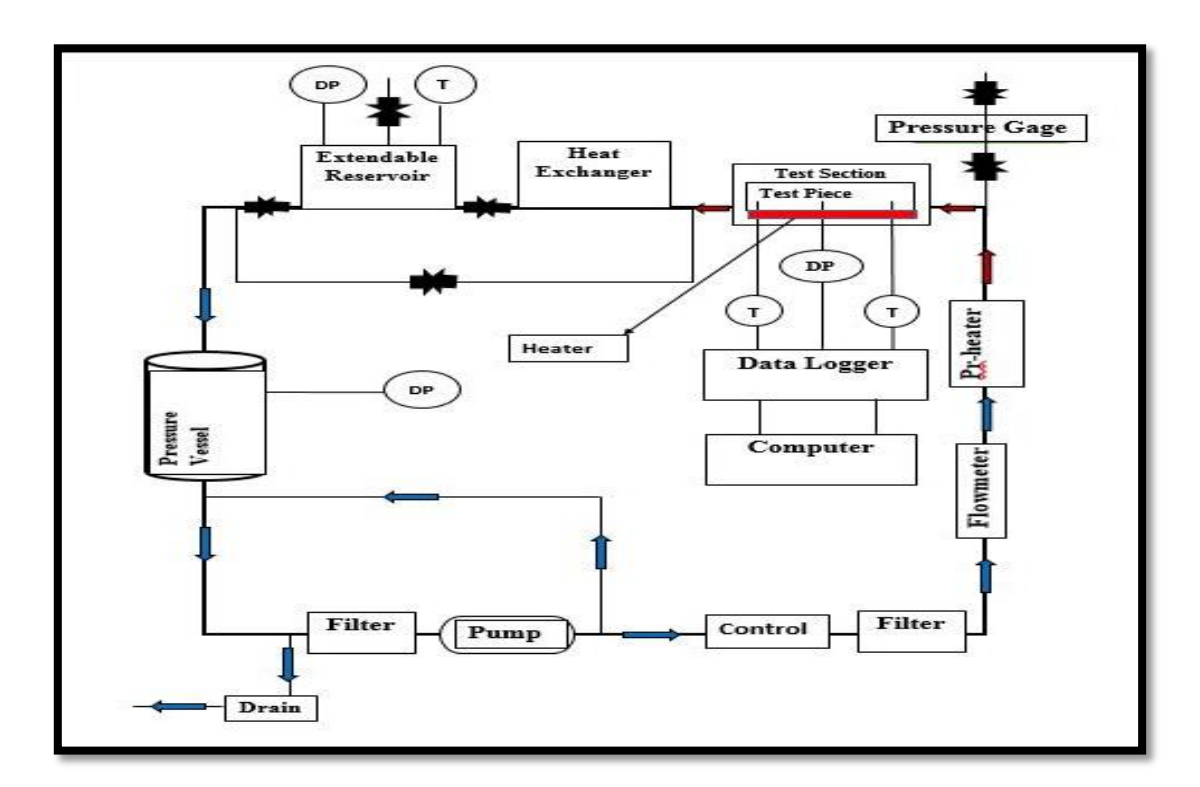


Figure (2): The Flow Loop

## Math and procedure

It appears that the Guess software utilized approximately two thousand heat transfer equations, which were later processed using Excel through iterative methods. As indicated in **Figure.1** the construction suggests that heat transmission occurs exclusively at the interface among the solid surfaces besides the R113 fluid. The arrangement of the two-dimensional array mainly influences the wall path, while the one-dimensional array is oriented perpendicular to the

R113 flow. Additionally, the two-dimensional array runs parallel to the R113 flow. The procedure outlined in **Figures.1** must be followed to accurately measure thermal conductivity. [4], [6].

$$\delta^2 T/\delta y^2 + \delta^2 T/\delta z^2 = 0 \tag{1}$$

Heat transfer calculations were performed using equation (3), which relied on the temperature (T) measured along the copper wall and in the y-direction, perpendicular to the R113 flow axis. This process added complexity to distributing the

(0.01 mm).

formula across the square area of the cell's zone

$$T_{i,i} = \delta y^2 (T_{i+1,i} + T_{i-1,i}) + \delta z^2 (T_{i,i+1} + T_{i,i-1}) / 2 (\delta y^2 + \delta z^2)$$
 (2)

The temperatures of the liquid, denoted as  $(T_L)$ , at any given axial location., [4],

$$T_{LT} = T_{in} + (Q_T/m_T C_{PT}) \tag{3}$$

To determine area of flow, [3],

$$A_T = \pi D_T^2 / 4 \tag{4}$$

The hydraulic diameter can be calculated, [3],

$$D_T = 4A_L/P \tag{5}$$

To compute the fluid of mean velocity by, [3],

$$U_{T} = m_{T}/\rho_{T} A_{T}$$
 (6)

To get  $(Re_T)$  can be seen in, [3],

$$Re_T = \rho_T U_T D_T / \mu_T \tag{7}$$

To find the  $(Pr_T)$  by, [3],

$$Pr_T = C_{pT}\mu_T/K_T \tag{8}$$

To get the  $(SS_T)$  by, [4],

$$SS_T = EE_{st}Re_T^{-0.205}Pr_T^{-0.503}$$
 (9)

To get the  $(EE_T)$  by, [4],

$$EE_T = -0.0225 \, exp^{\left(-0.0225 \, (\ln Pr_T)^2\right)} \tag{10}$$

To get the  $(Nu_T)$  by, [22],

$$Nu_T = 0.023 Re_T^{0.8} Pr_T^{0.4}$$
 (11)

To obtain the  $(\alpha_T)$  by, [4],

$$\alpha_T = \rho_T u_T C p_T S s_T \tag{12}$$

To get of fraction factor through,  $2000 < Re_T < 4000$ , [4],

$$FF = 0.0035 + (0.264/Re_T^{0.42})$$
 (13)

To get of fraction factor through,  $Re_T > 4000$ , [4],

$$FF = (3.6 \log 10(Re_T/7))^{-2}$$
 (14)

To obtain of (pressure drop) through, [4],

$$\Delta p_T = 2 * FF * L_T * \rho_T * {U_T}^2 / D_T \tag{15}$$

## **Results**

These Figure (3) represent the difference of the heat transmission coefficient (h) with respect to wall temperature (Tw) or distance from the inlet, under different mass flow rates. Each graph uses polynomial regression to predict the trend of the data points. General Trend in all four subplots (a, b, c, and d), the heat transfer coefficient increases with wall temperature. The relationship is modeled using a polynomial equation, and the fitted curves exhibit a strong correlation with the data (R2≈0.999), indicating high accuracy of the polynomial fit. Effect of Mass Flow Rate: Each plot corresponds to a different mass flow rate :( a) 0.01 kg/sec, (b) 0.0125 kg/sec. (c) 0.015 kg/sec, (d) 0.0175 kg/sec. As the mass flow rate increases, the heat transfer coefficient also increases for the same wall temperature range. This suggests enhanced convective heat transfer at higher flow rates due to increased fluid velocity and turbulence. Polynomial Equations: Each subplot contains a polynomial regression equation of the form, (h=aTw<sup>2</sup>+bTw+c). The coefficients (a, b, c) vary for each mass flow rate, demonstrating that the relationship between (h) and (Tw) is different depending on the flow rate. Practical Implications.

Higher mass flow rates result in improved heat transfer, which is crucial for applications like cooling systems, heat exchangers, and thermal management in engineering devices. The polynomial fits can be used for predictive modeling in heat transfer analysis. as shown in Figure (3).

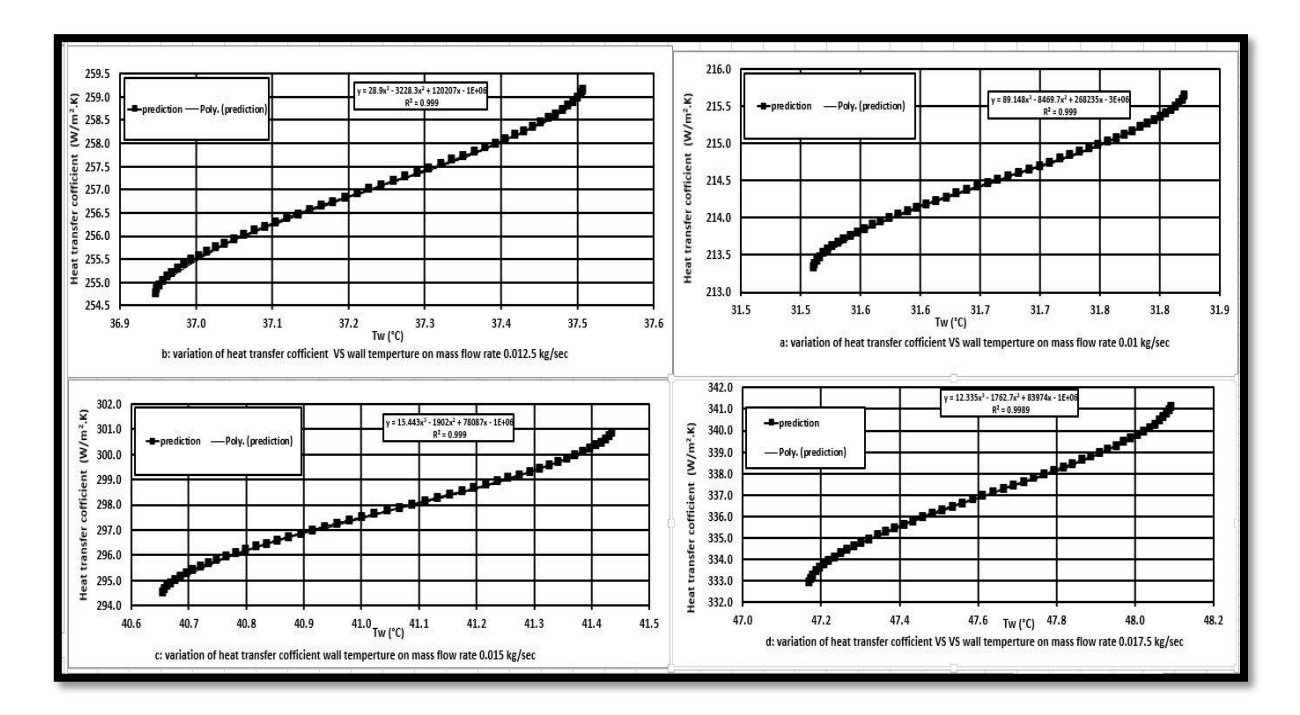


Figure (3): Heat transfer coefficient VS wall temperature

This Figure.4 presents four subplots showing the variation of fluid temperature along the tube's location at different mass flow rates. Each graph plots fluid temperature (°C) on the y-axis against distance from the plate or tube inlet (mm) on the xaxis. The data points represent predictions, and an exponential trend line is fitted to the data. Key observations: Subplot (a): Mass flow rate: 0.01 exponential equation: kg/sec, trend y=25.022e0.0002x,  $R^2 = 0.9998$ , indicating an excellent fit. Subplot (b): Mass flow rate: 0.0125 kg/sec, exponential trend equation: y=25.054e0.0003x,  $R^2 = 0.9996$ , also showing a very strong correlation. Subplot (c): Mass flow

rate: 0.015 kg/sec, exponential trend equation: y=25.082e0.0004x,  $R^2$ 0.9993, again demonstrating an excellent fit. Subplot (d): Mass flow rate: 0.0175 kg/sec, exponential trend equation: y=25.105e0.0004x,  $R^2$ = 0.9991,showing a very good match. Interpretation: The fluid temperature increases as it moves along the tube. The exponential equations indicate a very slow rise in temperature with distance. The rate of temperature increase appears slightly higher at higher flow rates. The R<sup>2</sup> values close to 1.0 indicate that the exponential model provides an excellent fit to the predicted data. as shown in Figure (4).

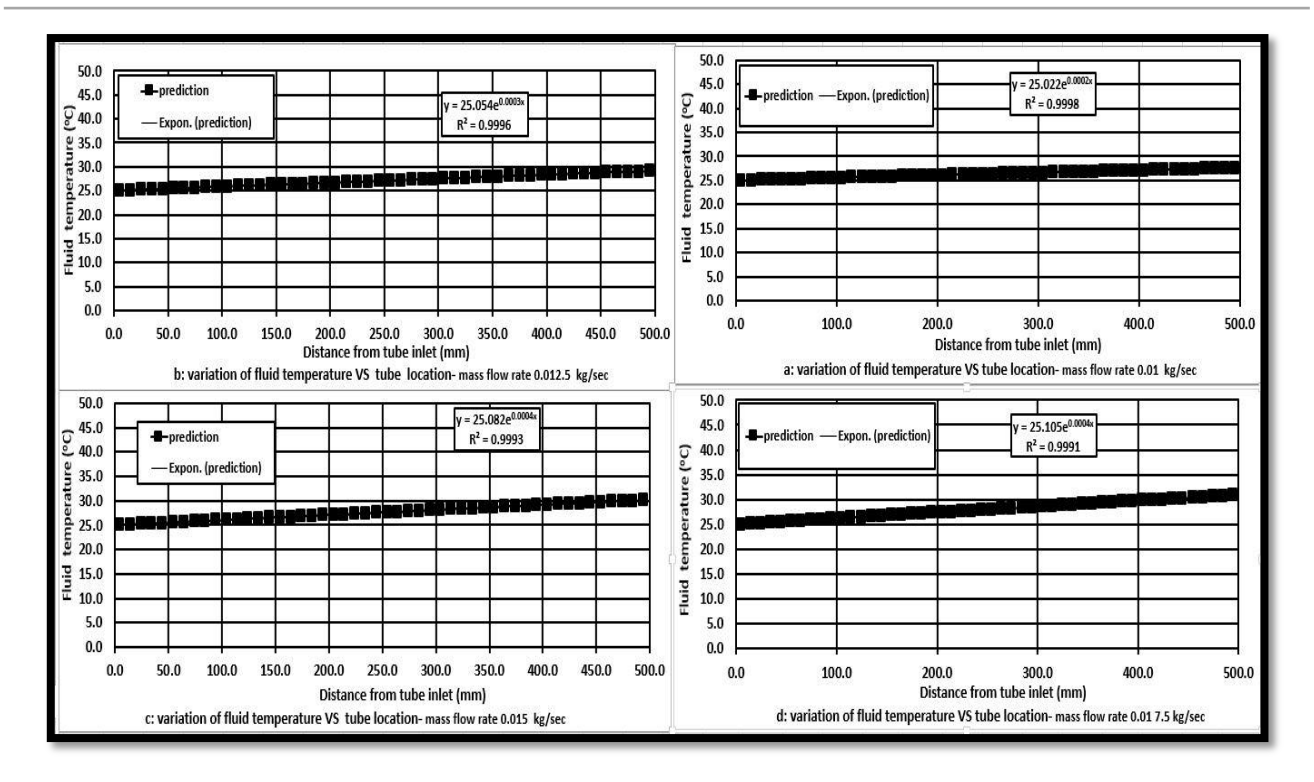


Figure (4): Fluid temperature VS location at different mass flow rates

The Figure (5) Appears to depict the variation of wall temperature as a purpose of the Reynolds number (Re) for different mass flow rates. The Reynolds number, a dimensionless parameter on liquid mechanics, predicts flow patterns across various liquid flow scenarios. The wall temperature is plotted against Re for four different mass flow rates: 0.01 kg/sec, 0.0125 kg/sec, 0.015 kg/sec, and 0.0175 kg/screech subplot (a, b, c, d) corresponds to a different mass flow rate and shows how the wall temperature changes with Re. The data points are fitted with polynomial equations (labeled as Prediction (Prediction)) .To model the relationship between

wall temperature and Re. The equations provided are polynomial fits of varying degrees, and the R<sup>2</sup> value of 1 indicates a perfect fit to the data points, which is unusual and might suggest overfitting or an error in the data or model. The wall temperature generally decreases as the Reynolds number increases, which could be indicative of enhanced cooling or heat transfer at higher flow rates. The specific trends and the degree of the polynomial fits suggest that the relationship between wall temperature and Re is complex and may involve multiple factors influencing heat transfer. as shown in Figure (5).

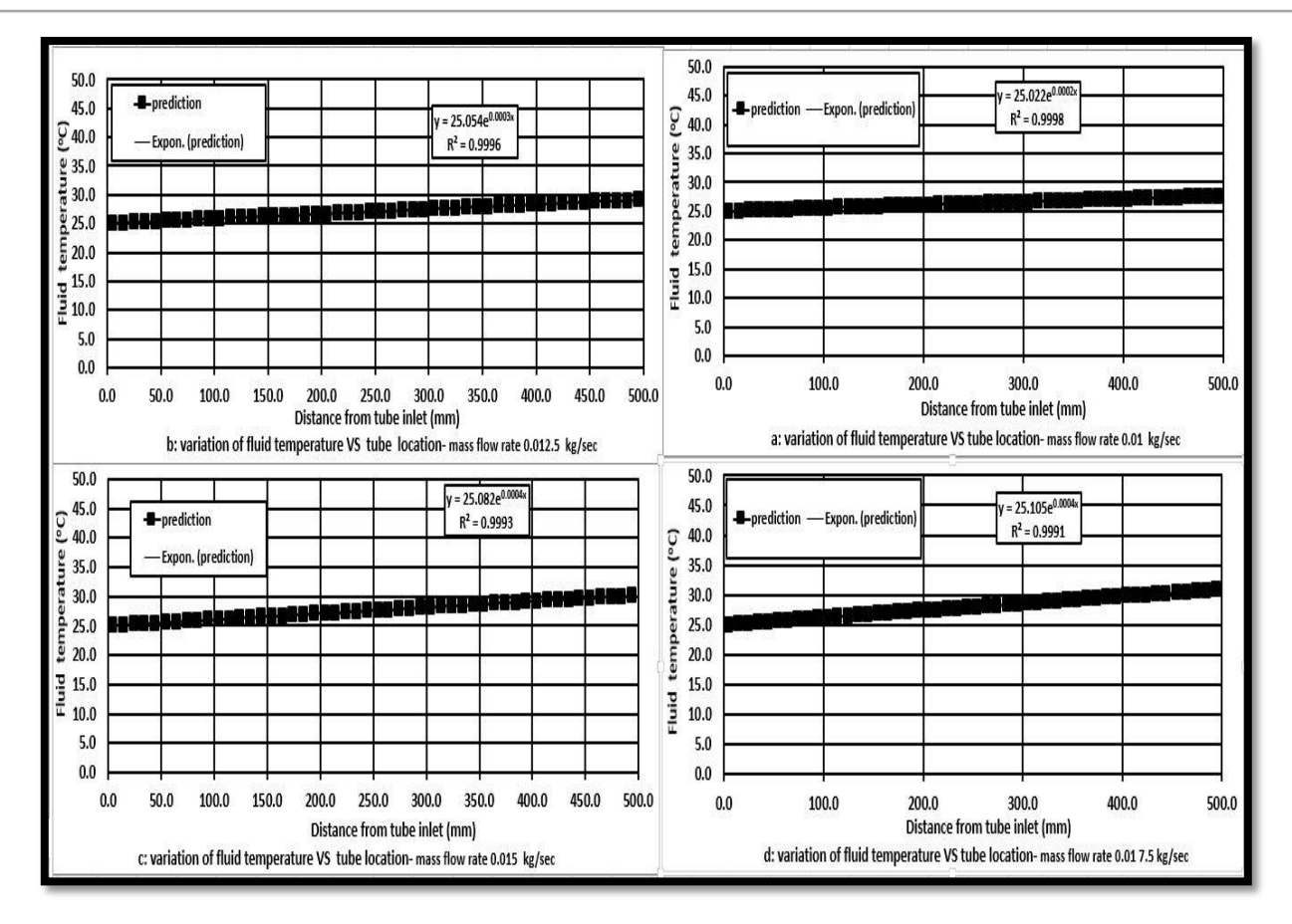


Figure (5): Wall temperature VS Re

The Figure (6) Appears to depict the variation of wall temperature along the length of a tube for different mass flow rates. Here's a breakdown of the components: Wall Temperature (°C): This is the temperature of the tube's wall, measured at various points along the tube's length. Distance from Tube Inlet (mm): This represents the position along the tube, starting from the inlet (0 mm) up to 600 mm. Mass Flow Rate: Different mass flow rates are considered, specifically 0.0125 kg/sec, 0.015 kg/sec, 0.01 kg/sec, and 0.0175 kg/sec. Each mass flow rate has a corresponding graph showing how the wall temperature changes along the tube. These equations are of the form V=ax6+bx5+cx4+dx3+ex2+fx+g, where V is the wall temperature and x is the distance from the

tube inlet. The R2=1 indicates a perfect fit of the polynomial to the data. Subplots: Subplot b: Shows the wall temperature variation for a mass flow rate of 0.0125 kg/sec. Subplot c: Shows the wall temperature variation for a mass flow rate of 0.015 kg/sec. Subplot c (second instance): Shows the wall temperature variation for a mass flow rate of 0.01 kg/sec. Subplot d: Shows the wall temperature variation for a mass flow rate of 0.0175 kg/sec. Each graph illustrates how the wall temperature changes as you move along the tube, with the temperature generally decreasing as the distance from the inlet increases. The polynomial equations provide a mathematical model to predict the wall temperature at any point along the tube for the given mass flow rates. as shown in Figure (6).

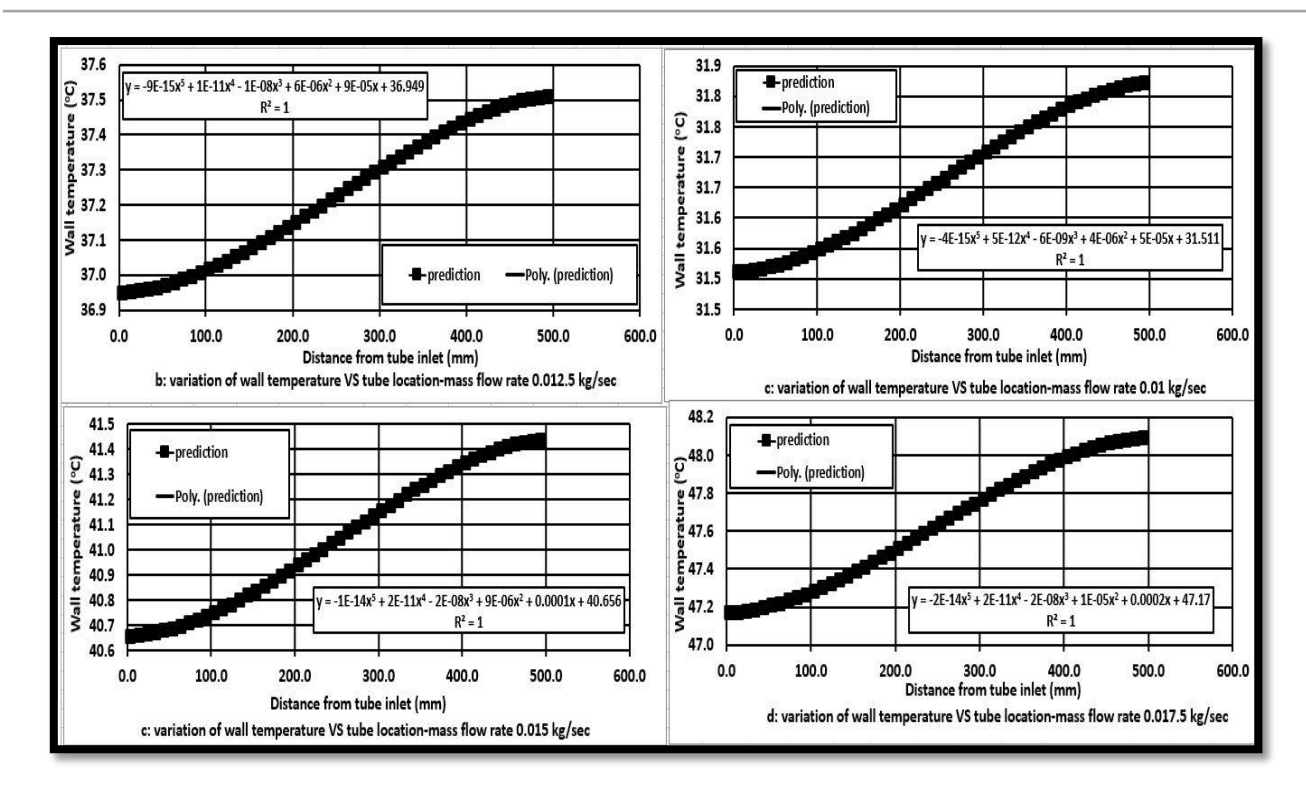


Figure (6): Wall temperature VS distance from tube inlet

The Figure (7) Presents the variation in fluid temperature along the length of a tube for different mass flow rates: 0.01 kg/sec, 0.0125 kg/sec, 0.015 kg/sec, and 0.0175 kg/sec. Each graph demonstrates how the fluid temperature changes as the distance from the tube inlet increases. Polynomial equations are provided for some

scenarios to model the relationship between the distance and fluid temperature, with an R2=1 indicating a perfect fit. Key observations: Fluid Temperature: Changes as the distance from the tube inlet increases, with specific trends for each mass flow rate, as shown in Figure (7).

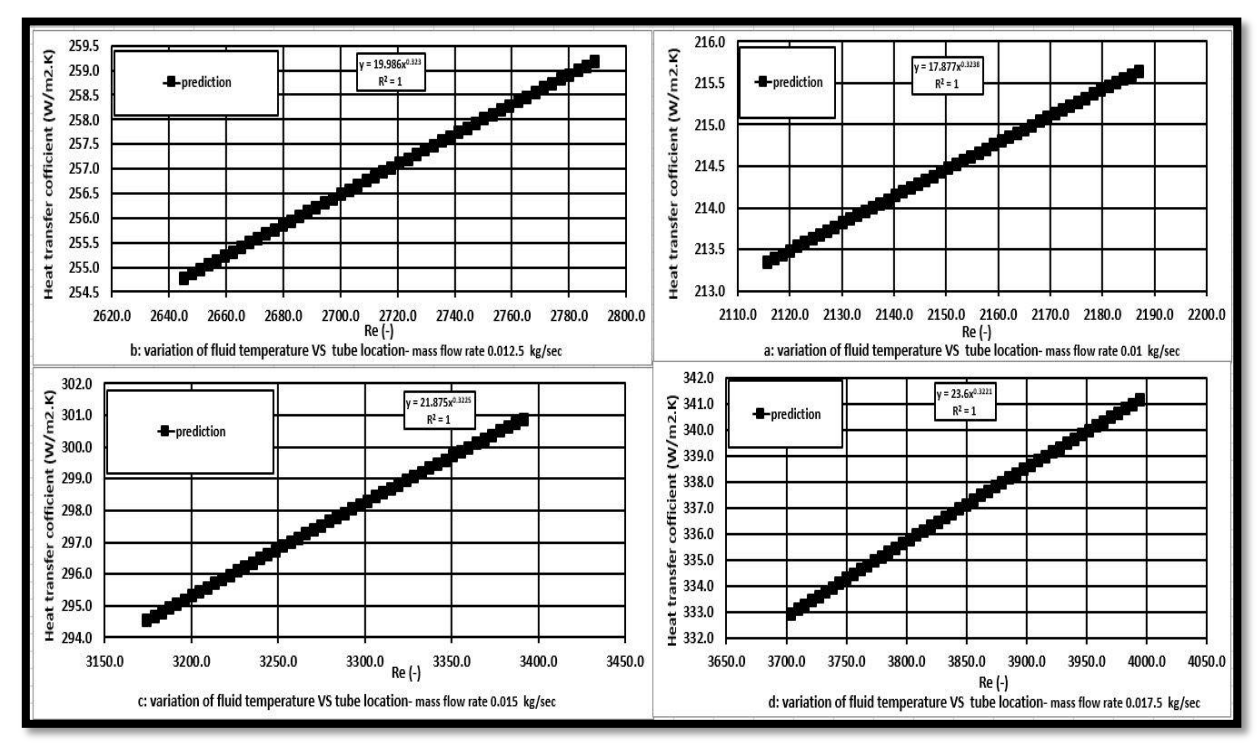


Figure (7): Liquid temperature against distance from pipe inlet

#### **Conclusions**

**Figure.3** illustrates a strong positive correlation between mass flow rate and heat transfer coefficient. The polynomial equations serve as reliable models for predicting heat transfer performance under varying conditions, making this information valuable for engineers designing thermal systems where convective heat transfer is crucial.

**Figure.4** depicts how fluid temperature varies along the tube at different mass flow rates. The results show that the temperature gradually increases with distance from the inlet, following an exponential trend with a minimal growth coefficient. Key observations include:

- Higher mass flow rates result in slightly elevated initial temperatures and a marginally steeper temperature rise.
- The overall temperature increase remains low, indicating efficient heat transfer characteristics.
- The exponential model provides an excellent fit for the predicted temperature data, with R<sup>2</sup> values exceeding 0.999, confirming the accuracy of the predictions. Overall, the figure suggests that while mass flow rate influences temperature distribution, the increase in temperature follows a consistent exponential trend.

**Figure .5** illustrates the relationship between wall temperature and Reynolds number for various mass flow rates, with polynomial fits modeling these trends. The findings suggest that higher Reynolds numbers correspond to lower wall temperatures, likely due to enhanced heat transfer at increased flow rates.

**Figure.6** presents the variation in wall temperature along the tube length for mass flow rates of 0.0125 kg/sec, 0.015 kg/sec, 0.01 kg/sec, and 0.0175 kg/sec. The graphs depict how wall temperature changes with increasing distance from the inlet, extending up to 500 mm. Key observations include:

- Wall temperature generally decreases as the distance from the inlet increases.
- Different mass flow rates produce distinct temperature profiles along the tube.
- Polynomial models predict wall temperature at any point along the tube, with  $R^2 = 1$  indicating a perfect fit.
- This data provides valuable insights into thermal behavior under different flow conditions, which is essential for heat transfer and fluid dynamics applications.

**Figure.7** highlights key trends in fluid temperature variations along the tube for different mass flow rates. Observations in results section:

#### References

- [1] A. F. Abed, M. J. Alshukri, A. M. Alsayah, R. H. Rasheed, and M. Khaled, "Numerical Investigation of Pyramid Solar Stills with PCM-Nanoparticles and Absorber Fins: Enhanced Thermal Performance for Sustainable Water Desalination," Heat Transf., 2024.
- [2] A. M. Alsayah, J. J. Faraj, and A. A. Eidan, "Improvements of heat transfer coefficient for thermosiphon heat pipe heat exchanger," in AIP Conference Proceedings, 2024, vol. 3105, no. 1.
- [3] B. K. Dutta, Heat transfer: principles and applications. PHI Learning Pvt. Ltd., 2023.

- [4] Holman, J. P. (2010).Heat Transfer, 10th Edition .New York, McGraw Hill, Inc., 1221, ISBN:978-0-07-352936-3, MHID: 0-07-352936-2.
- [5] R. S. R.SHAKIR, "Investigate the Flow of Boiling Heat Transfer in a Complex Geometry Flat Channel Investigate the Flow of Boiling Heat Transfer in a Complex Geometry Flat Channel," Univ. Thi-Qar J. Eng. Sci. مجلة جامعة , vol. 12, no. 1, pp. 21–25, 2022.
- [6] R. Shakir, "Prediction study of the boiling flow of heat transfer in an array of in-line micro-pin-fins heat sink," in AIP Conference Proceedings, 2023, vol. 2845, no. 1.
- [7] R. Shakir, "Boiling Heat Transfer in a Micro-Channel Complex Geometry," in IOP Conference Series: Materials Science and Engineering, 2020, vol. 928, no. 2, p. 22129.
- [8] R. Shakir, "Study Of Pressure Drop and Heat Transfer Characteristics Of Mini-Channel Heat Sinks," Iraqi J. Mech. Mater. Eng., vol. 22, no. 2, pp. 85–97, 2022, doi: 10.32852/iqjfmme.v22i2.595.
- [9] R. SHAKIR, "PREDICTION OF THE COEFFICIENT ON HEAT TRANSFER FOR HEAT TRANSFER FOR SINGLE-PHASE FLOW IN A ANNULAR PASSAGE ON VERTICAL TUBE BY FORCED CONVECTION HEAT FLOW," J. Optim. Decis. Mak., vol. 2, no. 2, pp. 297–303, 2023.
- [10] S. Algburi, A. M. Alsayah, M. A. Alkhafaji, and R. Shakir, "A comparison of single-phase of heat transfer in micro-channels and flat channel flows (guess study)," in AIP Conference Proceedings, 2025, vol. 3303, no. 1.
- [11] R. Shakir, "INVESTIGATION OF SINGLE-PHASE FLOW

- CHARACTERISTICS IN A STAGGER PIN-FINS COMPLEX GEOMETRY," J. Eng. Sustain. Dev., vol. 25, no. 6, pp. 74–81, 2021.
- [12] R. SHAKIR, "Investigate the Flow of Boiling Heat Transfer in a Complex Geometry Flat Channel," Univ. Thi-Qar J. Eng. Sci., vol. 12, no. 1, pp. 21–25, 2022.
- [13] R. Shakir, S. Algburi, and M. A. Alkhafaji, "The calculation of the heat path on the heat exchanger with the iteration method by using heat transfer equations (prediction study)," in AIP Conference Proceedings, 2025, vol. 3303, no. 1.
- [14] R. Shakir, "Boiling Heat Transfer in a Micro- Channel Complex Geometry," IOP Conf. Ser. Mater. Sci. Eng., vol. 928, no. 2, p. 22129, 2020, doi: 10.1088/1757-899X/928/2/022129.
- [15] R. SHAKIR, "GUESS HEAT TRANSFER COEFFICIENT OF FORCED CONVECTION FOR SINGLE-PHASE FLOW IN A SINGLE-PHASE PASSAGE ON A VERTICAL TUBE HEAT TRANSFER," J. Optim. Decis. Mak., vol. 2, no. 1, pp. 139–146, 2023.
- [16] R. Shakir, "Investigation of Single-Phase Flow Characteristics in an Inline Pin-Fins Complex Geometry," J. Phys. Conf. Ser., vol. 1879, no. 3, p. 32118, 2021, doi: 10.1088/1742-6596/1879/3/032118.
- [17] R. S. R.SHAKIR, "Pressure Drop Effect on Mini-Scale Heat Sink by Multi-phase: Review & Prediction Pressure Drop Effect on Mini-Scale Heat Sink by Multi-phase: Review & Prediction," Univ. Thi-Qar J. Eng. Sci. مجلة جامعة ذي قار للعلوم الهندسية, vol. 12, no. 1, pp. 15–20, 2022.
- [18] R. Shakir and R. SHAKIR, "Study on Heat Transfer and Pressure Drop through

- Different Channel Heights and Widths," Alkut Univ. Coll. J., vol. 2024, no. spacial issue, pp. 523–531, 2024.
- [19] S. Nashee and K. S. Mushatet, "Performance study on turbulent heat transfer using rectangular air duct integrated with continuous and intermittent ribs turbulators," Therm. Sci., no. 00, p. 214, 2024.
- [20] S. R. Nashee, "Enhancement of Heat Transfer in Nanofluid Flow Through Elbows

- with Varied Cross-Sections: A Computational Study.," Int. J. Heat Technol., vol. 42, no. 1, 2024.
- [21] S. R. Nashee, "Numerical Study for Fluid Flow and Heat Transfer Characteristics in a Corrugating Channel.," Int. J. Heat Technol., vol. 41, no. 2, 2023.
- [22] T. L. Bergman, Fundamentals of heat and mass transfer. John Wiley & Sons, 2011.